[논문] 한국소성·가공학회지, 제 32 권 제 1 호, 2023
Transactions of Materials Processing, Vol.32, No.1, 2023
http://data.doi.or.kr/10.5228/KSTP.2023.32.1.28

적층제조 연속섬유강화 고분자 복합재료의 물성 예측

P. Kahhal[1,2] · H. Ghorbani-Menghari[3] · 김형태[3] · 김지훈[4, #]

Prediction of the Mechanical Properties of Additively Manufactured Continuous Fiber-Reinforced Composites

P. Kahhal, H. Ghorbani-Menghari, H. T. Kim, J. H. Kim
(Received December 7, 2022 / Revised January 18, 2023 / Accepted January 19, 2023)

Abstract

In this research, a representative volume element (RVE)-based FE Model is presented to estimate the mechanical properties of additively manufactured continuous fiber-reinforced composites with different fiber orientations. To construct the model, an ABAQUS Python script has been implemented to produce matrix and fiber in the desired orientations at the RVE. A script has also been developed to apply the periodic boundary conditions to the RVE. Experimental tests were conducted to validate the numerical models. Tensile specimens with the fiber directions aligned in the 0, 45, and 90 degrees to the loading direction were manufactured using a continuous fiber 3D printer and tensile tests were performed in the three directions. Tensile tests were also simulated using the RVE models. The predicted Young's moduli compared well with the measurements: the Young's modulus prediction accuracy values were 83.73, 97.70, and 92.92 percent for the specimens in the 0, 45, and 90 degrees, respectively. The proposed method with periodic boundary conditions precisely evaluated the elastic properties of additively manufactured continuous fiber-reinforced composites with complex microstructures.

Keywords: Additive manufacturing, fiber reinforced composites, representative volume element, Periodic boundary condition, mechanical properties, micromechanical analysis.

1. Introduction

Additive manufacturing (AM) held the widespread attention of researchers recently and has been used in industrial applications such as electronics, biomedical, and aerospace [1-3]. Compared to traditional manufacturing techniques, additive manufacturing has advantages in materials waste reduction, process time saving, and complex geometrical design [4, 5].

To improve the performance of polymer composites, various reinforcements, such as carbon and Kevlar fibers, in continuous and chopped form, are combined with a thermoplastic matrix and then printed together. The remarkable strength to weight ratio of AM composites makes them very desired for industrial applications, presenting distinctive benefits over traditional composite manufacturing methods [6].

The AM carbon fiber composites has been widely researched. Brooks and Molony [7] designed parts for AM by aligning filaments adjacent to the load paths. Jiang et al. [8] optimized the fiber path of the AM composite utilizing solid orthotropic material penalization. Fernandes et al. [9] obtained the mechanical properties of an AM composite, Onyx, with two different continuous fiber infill patterns. Chacón et al. [10] investigated the effect of build orientation,

1. School of Mechanical Engineering, Pusan National University, Postdoctoral Researcher
2. Department of Mechanical Engineering, Ayatollah Boroujerdi University, Boroujerd, Assistant Professor
3. School of Mechanical Engineering, Pusan National University, Student
4. School of Mechanical Engineering, Pusan National University, Associate Professor
Corresponding Author: J. H. Kim, E-mail: kimjh@pusan.ac.kr
ORCID: 0000-0001-9334-0503

layer thickness, and fiber volume on the mechanical properties of AM composites.

The performance of these composites significantly depends on the fiber orientation [11]. Papa et al. [12] investigated the effect of fiber orientation on AM composites, utilizing tensile and compression tests, thermogravimetric analysis, and calorimetric analysis. Zhang et al. [13] examined build orientation and raster pattern effect on the fracture behavior of AM composites.

The finite element method (FEM) is effectively employed in frequent manufacturing fields as a potent tool to diminish experimental time and costs [14, 15]. For AM composites, the use of FEM has increased recently. Fernandes et al. [16] compared the experimental failure characteristics of the AM composites with finite element analysis using classical composite failure criteria. Kalova et al. [17] investigated the mechanical properties of a composite with a circular cross-section profile utilizing FEM and verified the results experimentally.

The representative volume element (RVE) method is useful for calculating the mechanical properties of composites using FEM. This method reflects the complicated micro-structures of composites and gives precise estimates [18].

In this work, an RVE-based FE Model is presented to estimate the mechanical properties of the composite with different fiber orientations. To construct the model, an ABAQUS Python script has been implemented to produce matrix and fiber in the desired orientations at the RVE. A script has also been developed to apply the periodic boundary conditions to the RVE. Experimental tests validated the analysis results.

2. Experiments

To investigate the effect of the fiber orientation on the mechanical properties of the printed composite, three different fiber angles have been considered. A desktop continuous carbon fiber 3D printer, Markforged Mark Two, was used to print the tensile test specimens. The printer can print thermoplastic parts with continuous fiber reinforcements using carbon, glass, and Kevlar fibers.

Two filament spools are used to print a continuous carbon fiber reinforced part. The first filament is composed of Nylon-based thermoplastic polymer with pre-blended carbon fiber reinforcement, or Onyx. The second strand is a roll of continuous carbon fiber coated with an adhesive. A cloud-based software package, Eiger, was used to modify cad geometry and input process parameters such as the layer height, filling percentage, type of reinforcement (fibers), and direction of fibers.

Tensile specimens were printed according to the standard test method (ASTM D3039) [19]. Different gripping tab conditions were used in the gripping area: carbon fiber reinforced plastics (CFRP), glass fiber reinforced plastics (GFRP), and no tab. Among them, the glued GFRP tabs had the best performance without slipping in the tensile test procedure.

Table 1 indicates the details of the tensile specimen printing.

Table 1 Details of the specimen printing.

Specimen geometry	ASTM D3039
Dimensions (mm)	250 × 15 × 1.75
No. of specimens	3 for each orientation
Fill pattern	Hexagonal
Fiber diameter (mm)	0.125
Fiber orientation (°)	0, 45, 90
Fiber fill type	Isotropic
Fill density (%)	37
Roof and floor layers	2
Wall layers	2
Print time (min)	90~110

Fig. 1 shows the fiber orientations of the specimens. Fig. 2 shows the experimental tensile test specimens.

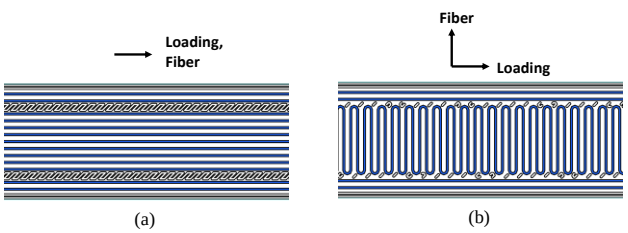

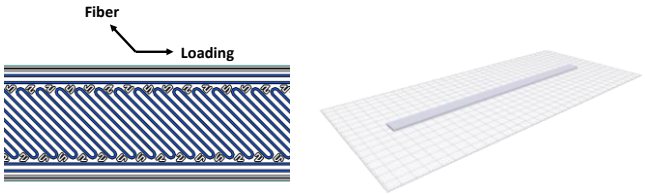

(c) (d)

Fig. 1 Fiber orientations of the specimens: a) 0 degree, b) 90 degrees, c) 45 degrees, and d) the 3D view of the tensile specimen

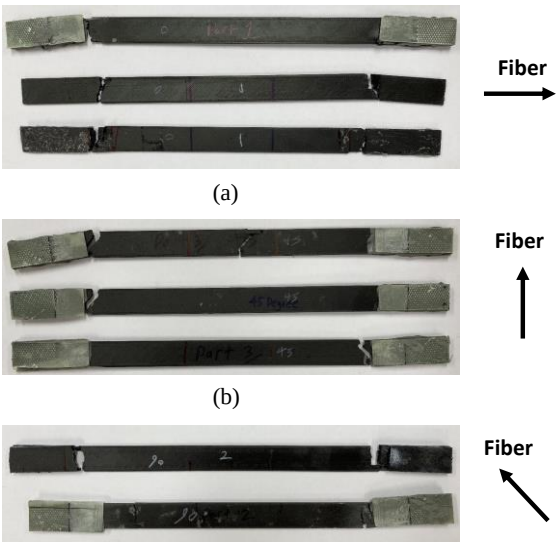

(a)

(b)

(c)

Fig. 2 Tensile test specimens: a) 0 degree, b) 90 degrees, c) 45 degrees.

Table 2 shows material properties of the RVE configurations [20].

Table 2 Material properties of the RVE configurations.

Material	Onyx	Carbon Fiber
Test (ASTM)	D638	D3039
Tensile Stress at Yield (MPa)	40	-
Tensile Strength (MPa)	37	800
Tensile Modulus (GPa)	2.4	60
Tensile Strain at Break (%)	25	1.5

3. Finite Element Model

An ABAQUS Python script has been used to generate AM specimen models and predict the elastic properties. Fig. 3 shows the RVEs for fiber angles of 0, 22.5, and 45 degrees and the meshed RVEs. Table 3 shows the RVE configurations. The RVE is composed of two materials: the continuous fiber and the matrix. The matrix material, or Onyx, was modeled as a homogeneous material because the find short fibers are randomly dispersed. In the RVEs, the two reinforcing fiber layers at the specimen boundaries aligned in the loading direction were not considered because the RVE width was much smaller than the specimen width.

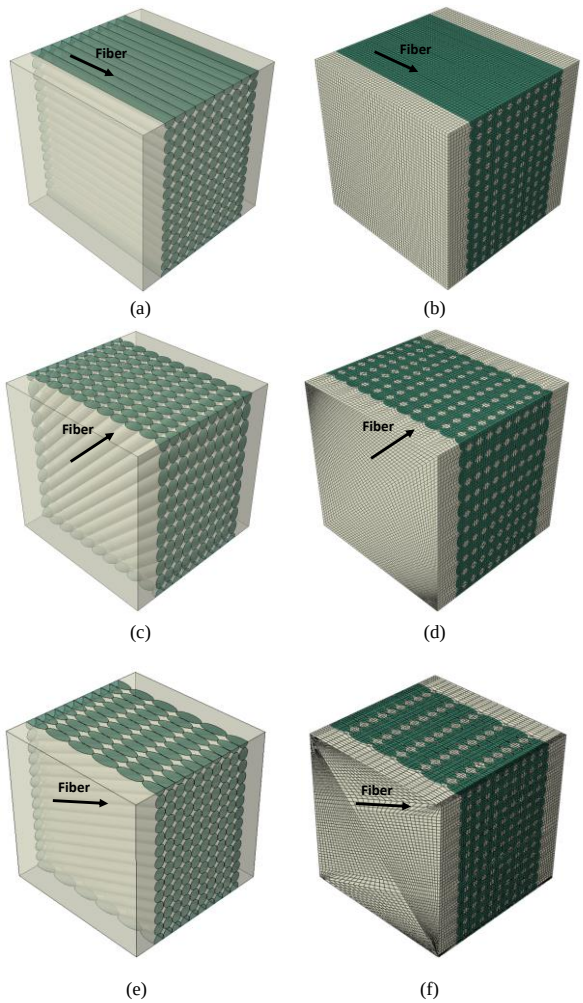

(a) (b)

(c) (d)

(e) (f)

Fig. 3 Implemented RVEs for different fiber orientations: a) 0 degree CAD model, b) 0 degree FE model, c) 45 degree CAD model, d) 45 degrees FE model, e) 22.5 degrees CAD model, and f) 22.5 degrees FE model.

Table 3 Details of the RVEs.

Fiber orientation (°)	0, 90	45	22.5, 67.5
Dimensions (mm^3)	1.77 × 1.77 × 1.75	1.77 × 1.77 × 1.75	1.77 × 1.77 × 1.75
Element type	C3D8R	C3D8R	C3D8R
No. of elements	289,520	319,896	279,382
Element size (μm)	32.5	32.5	32.5

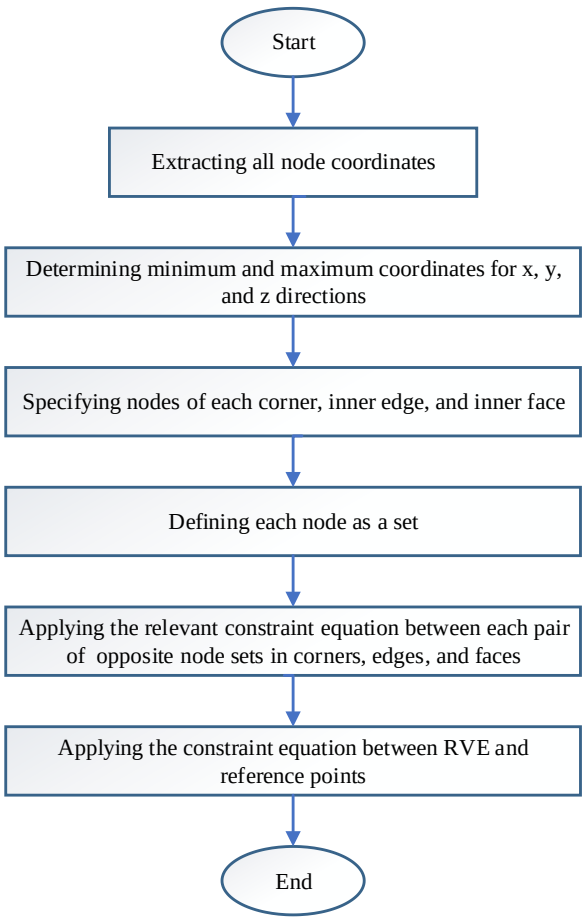

Fig. 4 Developed ABAQUS Python script flowchart for automatic application of PBCs.

Periodic boundary conditions (PBC) were applied to the RVEs [21]. The displacements for the periodic RVE can be expressed as [28]:

$$u_i^{k+} - u_i^{k-} = \varepsilon_{ij}^0 \left(x_j^{k+} - x_j^{k-} \right) \quad (1)$$

where u_i is the displacement, ε_{ij}^0 is the macroscopic strain, x_j is the coordinate. The indices $k+$ and $k-$ denote the kth pair of two opposite boundary surfaces of an RVE.

An ABAQUS Python script has been developed to automatically implement the PBC to any given RVE to apply periodic boundary conditions. Fig. 4 shows the developed Python script flowchart.

4. Results and Discussion

The effect of the fiber orientation on the mechanical properties of additively manufactured fiber reinforced composites was investigated using the micromechanical finite element method and experimental verification. Fig. 5 shows the stress-strain curves of the additively manufactured composites with different fiber orientations. Table 4 shows the prediction accuracy of Young's moduli of the additively manufactured composites at different fiber orientations. The predictions of 45 and 90 degree specimen showed good agreements with the measurements, while the accuracy is less for 0 degree specimen. The two reinforcing fiber layers at the specimen boundaries can cause the difference between FE models and experimental results. In addition, the inclusion of the nonlinearity of fiber and matrix properties may increase the prediction accuracy. Overall, the implemented micromechanical homogenization RVE can predict the elastic modulus in very good agreement with the experimental results.

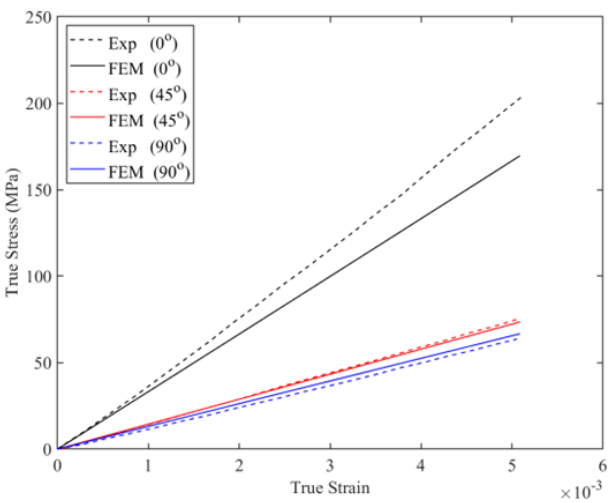

Fig. 5 stress-strain curves of the AM composites with different fiber orientations.

Table 4 Young's modulus of the additively manufactured composites with different fiber orientations.

Fiber orientation (°)	0	45	90
Measured Young's modulus (MPa)	39.81	14.79	12.54
FE Predicted Young's modulus (MPa)	33.34	14.45	13.15
Prediction accuracy (%)	83.73	97.70	92.92

Fig. 6 shows the variation of the Young's moduli with the fiber angles. The fiber angles of 22.5 and 67.5 degrees were also analyzed. The Young's modulus decreases with the increase of the fiber orientation angle, but did not show much difference when the fiber angle becomes larger than 45 degrees.

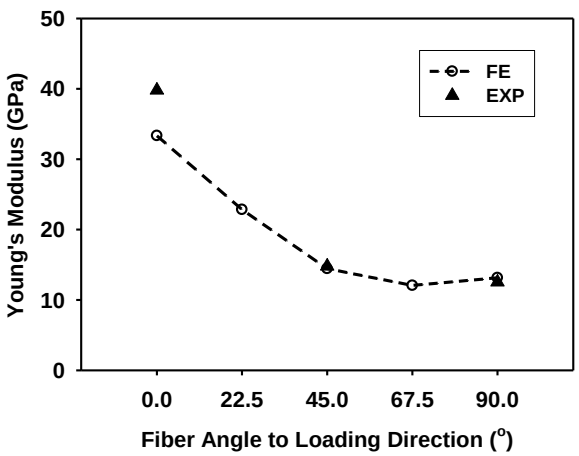

Fig. 6 Young's modulus variation with fiber angle to loading direction

Fig. 7 shows the Von-Mises stress distribution at the strain of 0.005 of the additively manufactured composites with different fiber orientations. Figs. 8 and 9 show the Von mises stress and logarithmic strain frequencies for different fiber orientations, respectively, at the strain of 0.005. The results show that the strain is homogeneous while the stress distribution splits into two in the 0 degree specimen because of the mechanical property difference of the fiber and matrix. For 45 and 90 degree specimens, high strains occur locally but the amount of stress distribution split decreases.

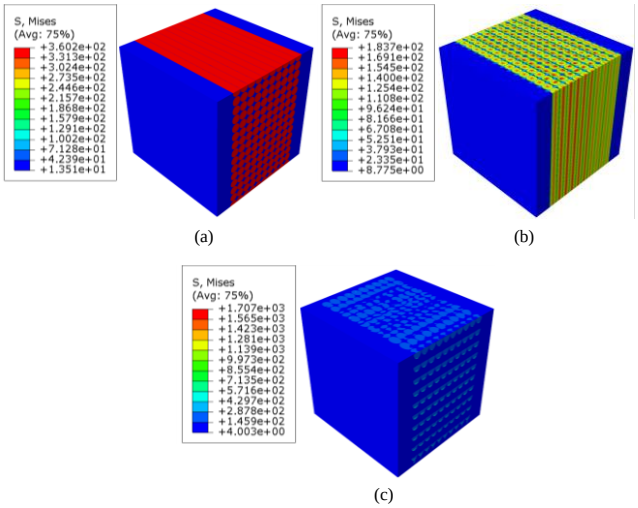

Fig. 7 Von-Mises stress distribution of the additively manufactured composites with different fiber orientations: a) 0 degrees, b) 45 degrees, and c) 90 degrees.

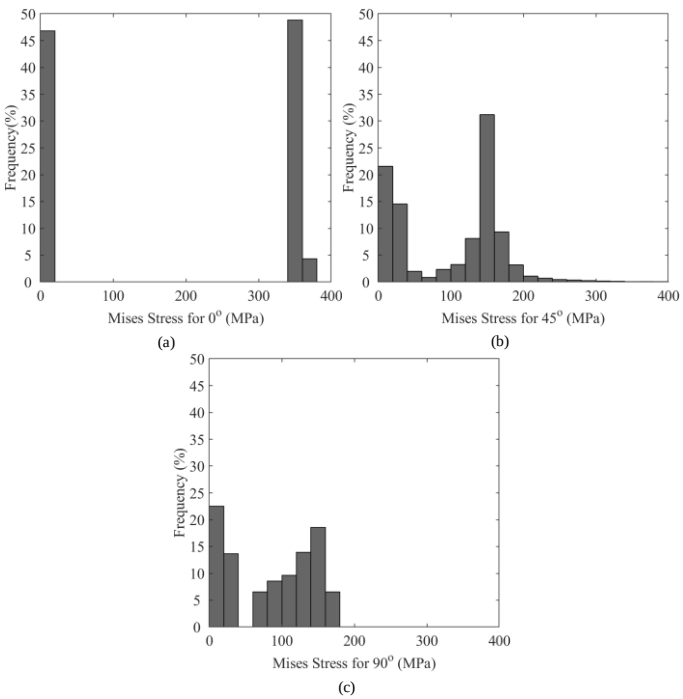

Fig. 8 Von-Mises stress frequencies of the additively manufactured composites with different fiber orientations: a) 0 degrees, b) 45 degrees, and c) 90 degrees.

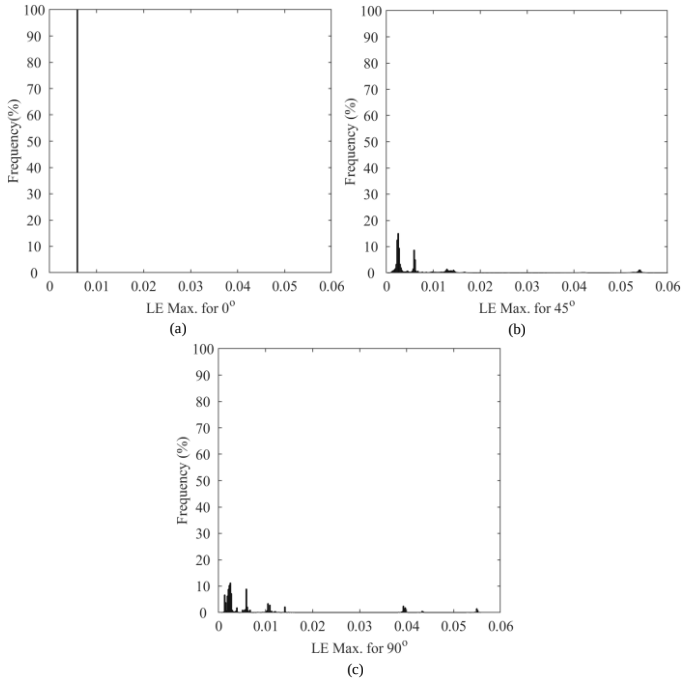

Fig. 9 Logarithmic strain frequencies of the additively manufactured composites with different fiber orientations: a) 0 degrees, b) 45 degrees, and c) 90 degrees.

5. Conclusion

A micromechanical homogenization RVE has been implemented to predict the mechanical properties of additively manufactured fiber-reinforced composites with different fiber orientations. The following conclusions are achieved:

(1) The implemented algorithms and scripts for RVE construction with fibers aligned at an angle and imposing periodic boundary conditions successfully generated RVE models for calculating mechanical properties of continuous fiber-reinforced composites.

(2) The prediction of the RVE-based FE analysis using periodic boundary conditions precisely predicted the elastic properties of composites with complex microstructures with good accuracy. It implies that the RVE-based finite element analysis can be used to predict the mechanical properties of the additively manufactured continuous fiber-reinforced composites.

ACKNOWLEDGEMENT

This work was supported by a 2-Year Research Grant of Pusan National University.

REFERENCES

[1] S.N. Economidou, D.A. Lamprou, D. Douroumis, 2018, 3D printing applications for transdermal drug delivery, Int. J. Pharm. Vol. 544, pp. 415~424. https://doi.org/10.1016/j.ijpharm.2018.01.031

[2] Y. Peng, Y. Wu, K. Wang, G. Gao, S. Ahzi, 2019, Synergistic reinforcement of polyamide-based composites by combination of short and continuous carbon fibers via fused filament fabrication, Compos. Struct. Vol. 207, pp. 232~239. https://doi.org/10.1016/j.compstruct.2018.09.014

[3] M. Invernizzi, G. Natale, M. Levi, S. Turri, G. Griffini, 2016, UV-Assisted 3D printing of glass and carbon fiber-reinforced dual-cure polymer composites. Mater. 9(7), 583. https://doi.org/10.3390/ma9070583.

[4] C.K. Chua, K.F. Leong, C.S. Lim, 2010, Rapid Prototyping: Principles and Applications, 3rd ed. Singapore: World Scientific Publishing Company.

[5] X. Wang, M. Jiang, Z.W. Zhou, J.H. Gou, D. Hui, 2017, 3D printing of polymer matrix composites: A review and prospective, Compos. B. Eng. Vol. 110, pp. 442~458. https://doi.org/10.1016/j.compositesb.2016.11.034

[6] R. R. Fernandes, N. van de Werken, P. Koirala, T. Yap, A. Y. Tamijani, 2021, M. Tehrani, Experimental investigation of additively manufactured continuous fiber reinforced composite parts with optimized topology and fiber paths, Addit. Manuf. Vol. 44, 102056. https://doi.org/10.1016/j.addma.2021.102056

[7] H. Brooks, S. Molony, 2016, Design and evaluation of additively manufactured parts with three-dimensional continuous fibre reinforcement, Mater. Des. Vol. 90, pp. 276~283. https://doi.org/10.1016/j.matdes.2015.10.123

[8] D. Jiang, R. Hoglund, D.E. Smith, 2019, Continuous fiber angle topology optimization for polymer composite deposition additive manufacturing applications, Fibre. Vol. 7, No. 2, 14. https://doi.org/10.3390/fib7020014

[9] R. R. Fernandes, A. Y. Tamijani, M. Al-Haik, 2021, Mechanical characterization of additively manufactured fiber-reinforced composites, Aerosp Sci Technol. Vol.

113, 106653. https://doi.org/10.1016/j.ast.2021.106653

[10] J.M. Chacón, M.A. Caminero, P.J. Núñez, E. García-Plaza, I. García-Moreno, J.M. Reverte, 2019, Additive manufacturing of continuous fibre reinforced thermoplastic composites using fused deposition modelling: Effect of process parameters on mechanical properties, Compos Sci Technol. Vol. 181, 107688. https://doi.org/10.1016/j.compscitech.2019.107688

[11] S. M. F. Kabir, K. Mathur, A. F. M. Seyam, 2020, A critical review on 3D printed continuous fiber-reinforced composites: History, mechanism, materials and properties, Compos. Struct. Vol. 232, 111476. https://doi.org/10.1016/j.compstruct.2019.111476

[12] I. Papa, A.T. Silvestri, M.R. Ricciardi, V. Lopresto, A. Squillace, 2021, Effect of Fibre Orientation on Novel Continuous 3D-Printed Fibre-Reinforced Composites, Polymers. Vol. 13, No. 15, 2524. https://doi.org/10.3390/polym13152524

[13] Z. Zhang, D. Yavas, Q. Liu, D. Wu, 2021, Effect of build orientation and raster pattern on the fracture behavior of carbon fiber reinforced polymer composites fabricated by additive manufacturing, Addit. Manuf. Vol. 47, 102204. https://doi.org/10.1016/j.addma.2021.102204

[14] P. Kahhal, J. Jung, Y.C. Hur, Y.H. Moon, J.H. Kim, 2022, Neural Network-Based Multi-Objective Optimization of Adjustable Drawbead Movement for Deep Drawing of Tailor-Welded Blanks, Mater. Vol. 15, 1430. https://doi.org/10.3390/ma15041430

[15] P. Kahhal, M. Yeganehfar, M. Kashfi, 2021, An Experimental and Numerical Evaluation of Steel A105 Friction Coefficient Using Different Lubricants at High Temperature, Tribol. Trans. Vol. 65, No. 1, pp. 25~31. https://doi.org/10.1080/10402004.2021.1966147

[16] R. R. Fernandes, A. Y. Tamijani, M. Al-Haik, 2021, Mechanical characterization of additively manufactured fiber-reinforced composites, Aerosp Sci Technol. Vol. 113, 106653. https://doi.org/10.1016/j.ast.2021.106653

[17] M. Kalova, S. Rusnakova, D. Krzikalla, J. Mesicek, R. Tomasek, A. Podeprelova, J. Rosicky, M. Pagac, 2021, 3D Printed Hollow Off-Axis Profiles Based on Carbon Fiber-Reinforced Polymers: Mechanical Testing and Finite Element Method Analysis. Polymers Vol. 13, No. 17, 2949. https://doi.org/10.3390/polym13172949

[18] W. Tian, L. Qi, X. Chao, J. Liang, M. Fu, 2019, Periodic boundary condition and its numerical implementation algorithm for the evaluation of effective mechanical properties of the composites with complicated micro-structures, Compos. B. Eng. Vol. 162, pp. 1~10. https://doi.org/10.1016/j.compositesb.2018.10.053

[19] Standard, A.J.A.D.D.M., 2008, ASTM D3039-Standard test method for tensile properties of polymer matrix composite materials. 3039.

[20] Markforged Material Datasheet: Composites, Rev 4.0 - 12/01/2020.

[21] W. Wu, J. Owino, A. Al-Ostaz, L. Cai, 2014, Applying Periodic Boundary Conditions in Finite Element Analysis. SIMULIA Community Conference, Providence, pp. 707~719.

[22] Suquet P., 1985, Elements of homogenization for inelastic solid mechanics. In: Sanchez-Palencia E, Zaoui A, editors. Homogenization techniques for composite media.Berlin, Heidelberg: Springer-Verlag, pp. 193~278.